


Layer-by-Layer 3D Constructs of Fibroblasts in Hydrogel for Examining Transdermal Penetration Capability of Nanoparticles

Journal of Laboratory Automation
1–7
© 2016 Society for Laboratory
Automation and Screening
DOI: 10.1177/2211068216655753
jala.sagepub.com


Xiaochun Hou^{1,2}, Shiyong Liu¹, Min Wang¹, Christian Wiraja¹,
Wei Huang², Peggy Chan³, Timothy Tan¹, and Chenjie Xu^{1,4}

Abstract

Nanoparticles are emerging transdermal delivery systems. Their size and surface properties determine their efficacy and efficiency to penetrate through the skin layers. This work utilizes three-dimensional (3D) bioprinting technology to generate a simplified artificial skin model to rapidly screen nanoparticles for their transdermal penetration ability. Specifically, this model is built through layer-by-layer alternate printing of blank collagen hydrogel and fibroblasts. Through controlling valve on-time, the spacing between printing lines could be accurately tuned, which could enable modulation of cell infiltration in the future. To confirm the effectiveness of this platform, a 3D construct with one layer of fibroblasts sandwiched between two layers of collagen hydrogel is used to screen silica nanoparticles with different surface charges for their penetration ability, with positively charged nanoparticles demonstrating deeper penetration, consistent with the observation from an existing study involving living skin tissue.

Keywords

artificial skin model, 3D printing, hydrogel, nanoparticles, transdermal delivery

Introduction

Nanoparticle (NP)-based transdermal drug delivery systems have attracted great interest due to their abilities to assist drug penetration across the skin layers while providing protection against the destructive local environment.¹ These transdermal nanomaterials can exist in the form of micelles, liposomes, gold NPs, and so forth.² Recent research suggests that the skin penetration efficacy and efficiency of these nanomaterials are related to their size and surface properties.^{3–5} The best way to examine these parameters is by testing candidate NPs directly with living human skin tissue or animal models, especially a porcine model. However, living human skin tissue is not always available, and its usage is subject to ethical regulation as well. On the other hand, animal experiments are costly and time-consuming.⁶

Bioprinting technology is emerging as a powerful tool for building tissues for drug discovery and regenerative medicine purposes. Based on the latest development in medical imaging, material science, and three-dimensional (3D) printing, bioprinting builds 3D tissue structures by simultaneously depositing live cells and growth factors along with biomaterial scaffolds at designated locations to mimic native tissue architecture and formation process.⁷ Matsusaki and his colleagues constructed 3D cellular multilayers that include cells and fibronectin-gelatin nano-extracellular matrix (ECM) films

using layer-by-layer deposition technology.⁸ Taking this concept, researchers have constructed 3D skin tissues using layer-by-layer deposition of collagen matrices, keratinocytes, and fibroblasts to construct both epidermal and dermal compartments. Importantly, the artificial models were shown to be morphologically and biologically representative of in vivo human skin tissue.^{9–11}

Inspired by these pioneering works, our goal is to explore the utilization of a 3D-printed skin model to examine transdermal penetration abilities of NPs and create a simple platform for rapid screening of transdermal NPs. As a proof-of-concept study, a simplified 3D skin tissue was constructed by printing

¹School of Chemical and Biomedical Engineering, Nanyang Technological University, Singapore

²Key Laboratory for Organic Electronics and Information Displays, Nanjing University of Posts and Telecommunications, Nanjing, China

³Faculty of Science Engineering & Technology, Swinburne University of Australia, Hawthorn, Australia

⁴NTU-Northwestern Institute for Nanomedicine, Nanyang Technological University, Singapore

Received April 9, 2016.

Corresponding Author:

Chenjie Xu, School of Chemical and Biomedical Engineering, Nanyang Technological University, 62 Nanyang Drive, 637459 Singapore.
Email: cjxu@ntu.edu.sg

blank collagen layer and fibroblast cells alternately in a layer-by-layer fashion. Valve on-time was found to have a significant effect over the morphology of the printed pattern. After examining the swelling of printed 3D collagen scaffolds in cell culture medium, we further examined the viability of fibroblasts in the printed construct. Finally, the optimized system was used to examine the influence of surface charge of silica NPs to their penetration ability (Fig. 1). The work presented here sets the stage for the further development and application of 3D skin tissue that combines the latest development of manufacturing, materials, and cell biology.

Materials and Methods

Collagen (rat tail, type I) was purchased from BD Biosciences (San Jose, CA). Dulbecco's modified Eagle's medium (DMEM) with high glucose (4.5 g/L) and L-glutamine, fetal bovine serum (FBS), penicillin-streptomycin (10,000 U/mL), and trypsin-EDTA (0.5%, 10 \times) were obtained from Gibco Life Technologies (Carlsbad, CA). NucBlue Live ReadyProbe Reagent, fluorescein diacetate (FDA), and propidium iodide (PI) were purchased from Life Technologies. Qtracker 565 and 655 Cell Labeling Kits and DiO (3,3'-dioctadecyloxycarbocyanine perchlorate) were obtained from Molecular Probes by Life Technologies. Polystyrene (hydroxyl polystyrene NPs), amine-modified polystyrene (amine polystyrene NPs), and sulfate-modified polystyrene (sulfate polystyrene NPs) latex beads were purchased from Sigma-Aldrich (St. Louis, MO). Rhodamine B isothiocyanate was obtained from Sigma-Aldrich. Primary dermal fibroblasts (3T3, normal, and human adults) were purchased from ATCC (Manassas, VA). All other chemicals without special description were from Sigma-Aldrich.

Overview of 3D Printing Machine

The layer-by-layer 3D construct is fabricated using a 3D Discovery Instrument (RegenHU Ltd., Villaz-St.-Pierre, Switzerland) (Suppl. Fig. S1). The instrument consists of a three-axis positioning system with a tool changer and a building platform used to fix different substrate types. All four print heads are valve based. The liquid material is dispensed by pneumatic pressure during the gate-opening phase of the microvalves. The volume of dispensed droplets was manipulated by controlling valve on-time and air pressure. Printing parameters (valve on-time, dosing distance, extruder feed rate, and needle length) were manipulated by the 3D Discovery HMI (human-machine interface).

Printing 3D Construct of Collagen Hydrogel

The collagen stock was diluted to 4.0 mg/mL with 1 \times Dulbecco's phosphate-buffered saline (PBS; without calcium

chloride and magnesium chloride) and 0.02 N acetic acid ($\geq 99.85\%$). This solution was maintained at 4 °C until it was loaded into the cartridge for printing. The dimensions of the 3D construct were 1.5 \times 1.5 cm², and it was fabricated by printing the collagen solution prepared above in a layer-by-layer fashion. Specifically, after one layer of collagen was printed, 10 μ L of sodium bicarbonate (NaHCO₃) solution (0.208 M) was immediately added onto the surface of the collagen layer to induce gelation, which took approximately 1 min. Then the next layer of collagen was printed and gelated with NaHCO₃ solution and so on. Finally, the construct was examined with an optical microscope. During the printing of blank collagen, the valve on-time was set in the range of 8000–8500 μ s. Air pressure was fixed at 2.8 bar (0.28 MPa). The diameter of the nozzle orifice was 0.25 mm.

Printing 3D Constructs of Fibroblast-Laden Hydrogel

3T3 fibroblasts were cultured at 37 °C in 5% CO₂ in DMEM supplemented with 10% FBS and 1% penicillin-streptomycin. Culture medium was exchanged every 3 days, and cells were passaged when they reached 80% confluence in a 75 cm² cell culture flask. Before printing, cells were stained with Qtracker and trypsinized using 0.05% trypsin. Briefly, 1 μ L of Qtracker Component A and 1 μ L of Component B were mixed in a 1.5 mL tube and incubated for 5 min at room temperature before being diluted with 1 mL of fresh complete growth medium. Then this solution was added into the plate containing fibroblasts. After an overnight incubation, cells were rinsed twice with PBS and trypsinized for printing.

To fabricate 3D constructs of fibroblast-laden hydrogel, one layer of collagen with dimensions of 1.5 \times 1.5 cm² was first printed and gelated with NaHCO₃ solution. This step is the same as during the fabrication of the 3D collagen hydrogel scaffold. Subsequently, cell suspension (1 \times 10⁶/mL) in complete culture medium was dispersed on the surface of the collagen layer. The construct was immediately placed in a cell incubator (37 °C, 5% CO₂) for 30 min to allow the attachment of cells onto the collagen hydrogel. Then the third layer (i.e., collagen layer) was printed on the cell layer. And the fourth layer (i.e., cells) came above the third layer. These steps were repeated until the desired construct was achieved. Finally, the 3D construct was placed in the cell incubator (37 °C, 5% CO₂) for 1 h to allow collagen gelation to complete before the complete culture medium was added. The visualization of cells in the construct relied on a confocal microscope (Zeiss LSM 700), which used a 405 nm laser as the excitation wavelength for Qtracker 565 (emission 534–600 nm) and Qtracker 655 (emission 620–681 nm). The images were collected as Z stacks with a step size of 12.30 μ m and processed using Zeiss LSM software. The average cellular fluorescence intensity was quantified

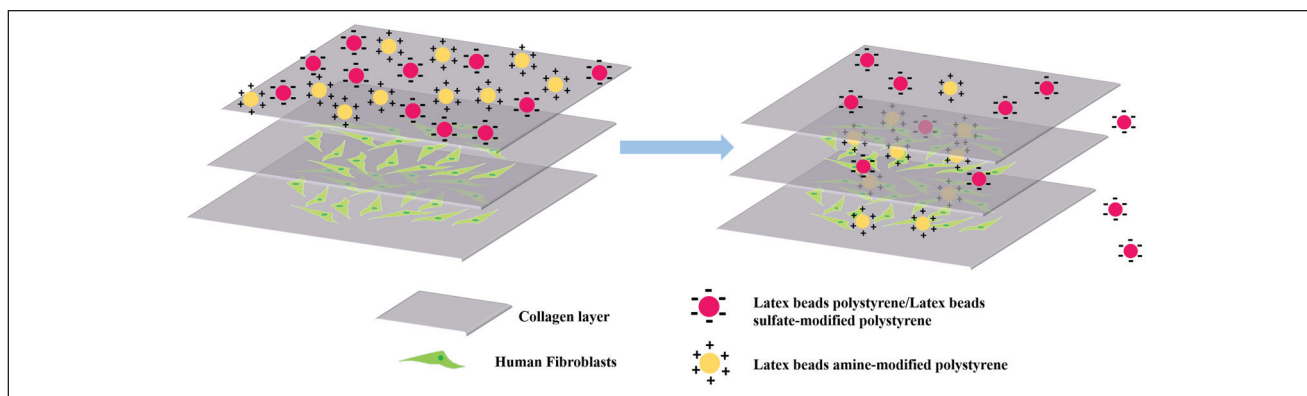


Figure 1. The 3D construct is fabricated by layer-by-layer deposition of collagen and fibroblasts. It partially mimics functions of skin and provides a simple platform for the rapid screening transdermal penetration ability of NPs.

with ImageJ. The valve on-time was 8300 μ s for printing collagen and 6000 μ s for dispersing cell suspension. Air pressure was set at 2.8 bar (0.28 MPa). The diameter of the nozzle orifice was 0.25 mm.

Cell Viability Analysis

The viability of cells in the 3D construct was examined using NucBlue Live ReadyProbe Reagent (Hoechst 33324), FDA, and PI. Specifically, the 3D construct was maintained in cell culture medium for 7 days and the media was changed every 3 days. Seven days later, the media was replaced with fresh media containing Hoechst 33324 (2 drops/mL), 5 mg/mL FDA, and PI (2 drops/mL). After 5–10 min of incubation at room temperature, the construct was washed twice with PBS before being imaged with a confocal microscope (Zeiss LSM 700) using a 405 nm laser for Hoechst 33324, 488 nm laser for FDA, and 514 nm laser for PI. The images were collected as Z stacks with a step size of 100 nm and processed using Zeiss LSM software. The live and dead cells were quantified through ImageJ. The ratio of viable cells to the total number of cells was expressed as the viability.

Silica NP Penetration Assay with 3D Construct

The 3D construct was printed as described above except that fibroblasts were pre-labeled with DiO.¹² The printed construct was placed in the incubator for 1 h to allow the gelation before being placed in the culture media. Then polystyrene beads were added to the media with a concentration of 0.1 mg/mL. After 3 h of incubation, the construct was gently washed with PBS twice and placed in fresh medium before being imaged with a confocal microscope. The images were collected as Z stacks with a step size of 100 nm and processed using Zeiss LSM software. The average cellular fluorescence intensity was quantified with ImageJ.

Results and Discussion

Optimization of Valve On-Time

Collagen type I is selected as the building material of the 3D construct because it is a major component of the ECM that provides tensile strength and elasticity to the skin.^{13,14} The 3D Discovery Instrument used in this study is based on a valve-based printing technique and has the advantage of being one of the gentlest techniques for printing any number of cells.¹⁵ Another advantage of this technique is the ability to alter the volume of bioink dispensed in each droplet through modifying the diameter of the nozzle orifice, the valve on-time, or the inlet pressure. The change of droplet volume was reflected by the width change of the printed collagen hydrogel line. The smallest available nozzle orifice chosen was 0.25 mm, and the inlet pressure was fixed at 0.28 MPa, which left the valve on-time as the only remaining factor to alter the droplet size. An experiment was devised to characterize the variation of the width of the printed collagen hydrogel line over a range of valve on-times for the hydrogel pattern illustrated in **Figure 2a**. As shown in **Figure 2b,c**, a longer valve on-time resulted in a wider hydrogel line. Specifically, when the valve on-time increased from 8000 to 8400 μ s, the width of the hydrogel line increased from 526 to 730 μ m, while the gap between hydrogel lines decreased from 275 to 78 μ m. To maximize line width while still maintaining gaps between the hydrogel line and valve on-time was set at 8300 μ s for the rest of the project.

Fabrication of Multilayered Collagen Hydrogel Constructs

Second, we explored the stability of the printed 3D collagen constructs. With the optimized valve on-time and other fixed parameters, three kinds of collagen constructs containing one, four, or seven layers of collagen were fabricated (**Fig. 3a**)

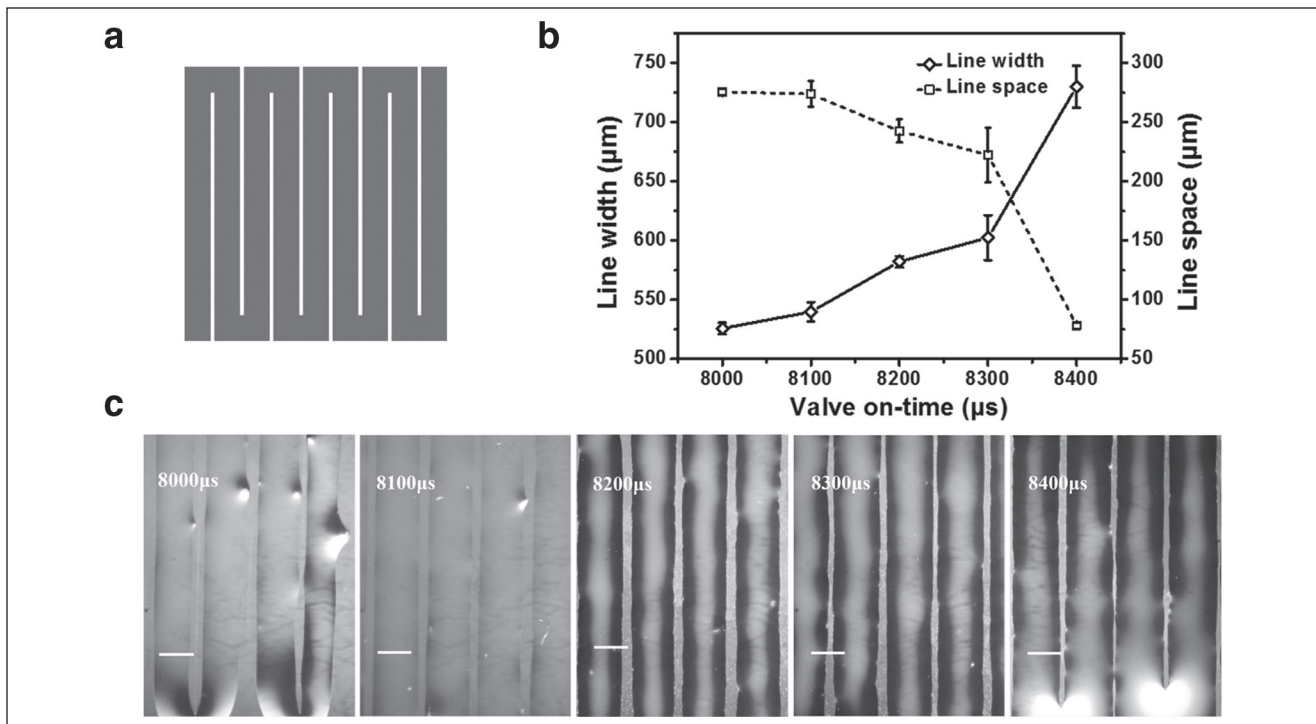


Figure 2. Impact of valve on-time on the collagen hydrogel line. (a) Illustration of the printed hydrogel pattern. (b) Quantification of the width and spacing of the hydrogel lines in c. (c) Line of collagen hydrogel printed by 3D bioprinter. During printing, valve on-time was tuned from 8000 to 8400 μs while all other parameters were fixed. Scale bar: 500 μm .

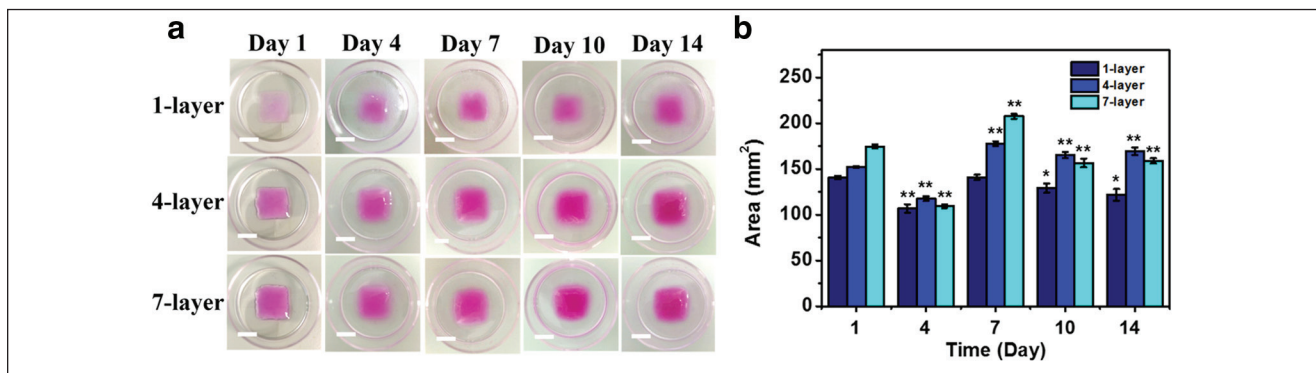


Figure 3. Swelling of 3D collagen constructs with one, four, and seven layers of collagen in the complete cell culture medium during a 14-day incubation. (a) Representative images of 3D collagen constructs from 1 to 14 days. Scale bar: 1 cm. (b) Quantification of the area of 3D collagen construct covered during the 14-day incubation. One-way ANOVA with post hoc Tukey HSD test was applied for calculation between areas on days 4, 7, 10, and 14 with day 1. * $p < 0.05$, ** $p < 0.01$.

using layer-by-layer printing together with the timely gelation. To allow visualization and quantification of the construct, rhodamine B isothiocyanate was used to dilute the collagen stock as the printing solution for day 1 of one, four, and seven layers. As shown in the day 1 images in **Figure 3a**, the color of the 3D constructs became deeper when there were more layers of collagen. Later, these constructs were placed in the complete cell

culture medium for 14 days, and the color is the phenol red of the cell culture medium from days 4 to 14. Their swelling was quantified through measuring the area they covered on the petri dish (**Fig. 3b**). During the 14-day period, there was minimal change of the area of collagen construct covered for all three samples, which demonstrates the stability of these scaffolds.

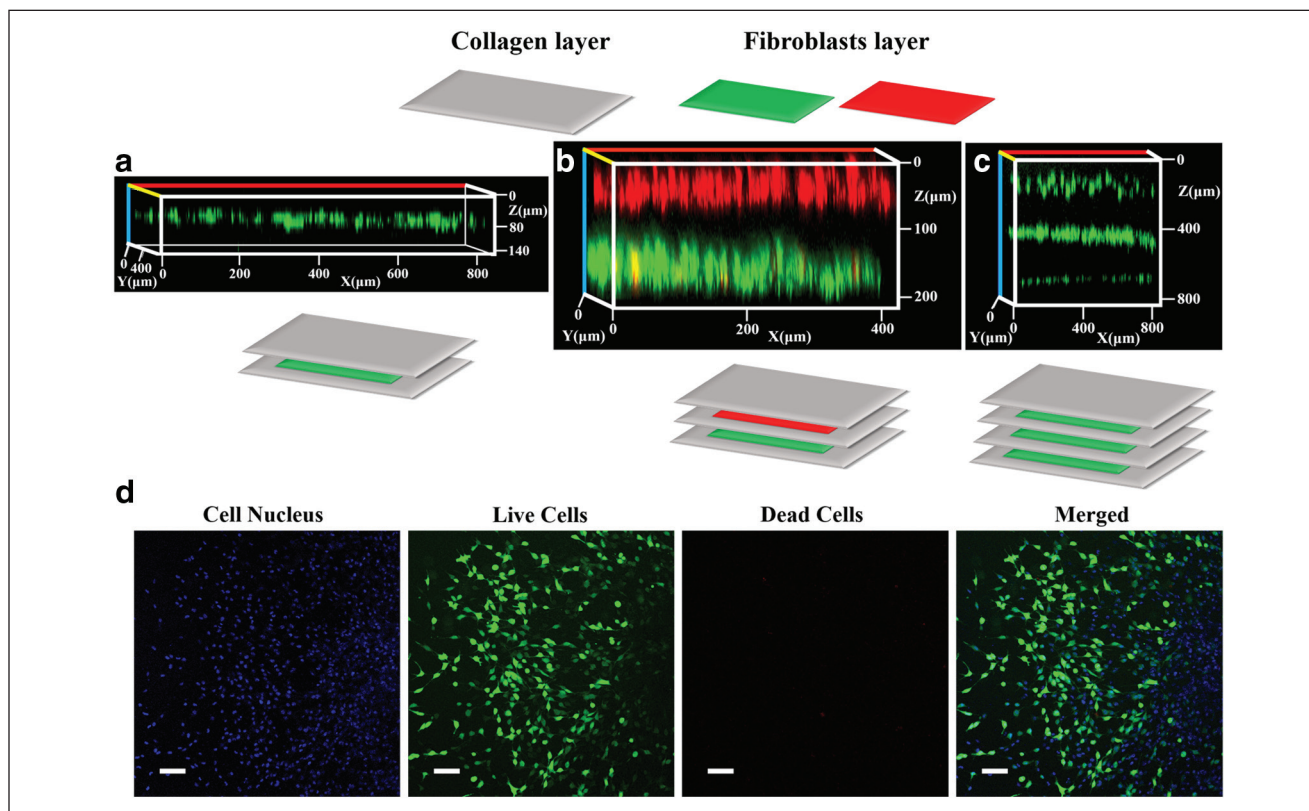


Figure 4. 3D constructs of fibroblasts in collagen. (a) Schematic and confocal image of 3D construct containing two layers of collagen and one layer of Qtracker-labeled fibroblast layers. (b) Schematic and confocal image of 3D construct containing three layers of collagen and two layers of Qtracker-labeled fibroblast layers. (c) Confocal image of 3D construct containing four layers of collagen and three layers of Qtracker-labeled fibroblast layers. Cut lines: X-red, Y-green, Z-blue. (d) Cell viability was assessed at the three-layer scaffold after being cultured for 7 days. The nuclei of human fibroblasts were labeled with NucBlue Live ReadyProbe Reagent (blue), FDA for live cells (green), and PI for dead cells (red). Scale bar: 200 μm .

Fabrication of 3D Constructs of Fibroblasts in Collagen

3D constructs of fibroblasts in collagen were fabricated by printing collagen layers and cell layers alternatively. The cells were prestained with either Qtracker 565 or Qtracker 655 before printing, and the construct was cultured for 24 h in a humidified incubator before being imaged with a confocal microscope.

As shown in **Figure 4a–c**, the cell layer was nicely sandwiched by the collagen layers in all three constructs despite their different thickness (three, five, or seven layers). After printing, no cell penetration into the collagen layer was observed. The thickness of the collagen layer was found to be 150 μm through measuring the distance between two cell layers in the confocal images.

The viability of cells within the construct was examined through FDA/PI staining. Taking the three-layer construct (**Fig. 4a**) as an example, we examined the viability of encapsulated fibroblasts after 7 days of culturing. As shown in **Figure 4d**, more than 95% of the cells remained viable

after the 7 days of culturing, which indicates sufficient nutrient diffusion into the collagen from the culture medium. A similar phenomenon (**Suppl. Fig. S2**) was also observed on the five-layer scaffold, in which both layers of fibroblasts in the scaffold showed high cell viability and good cellular morphology.

3D Constructs of Fibroblasts in Collagen for Examining the Skin Penetration Capability of NPs

This 3D construct was then applied to examine the skin penetration ability of various NPs. As mentioned above, the skin penetration efficacy and efficiency of these NPs are related to their surface properties. Thus, we examined polystyrene NPs with the same size but different surface properties to evaluate their penetration ability. Specifically, the 3D construct containing one layer of fibroblasts sandwiched between two collagen layers was placed into the culture medium containing three kinds of polystyrene NPs of the

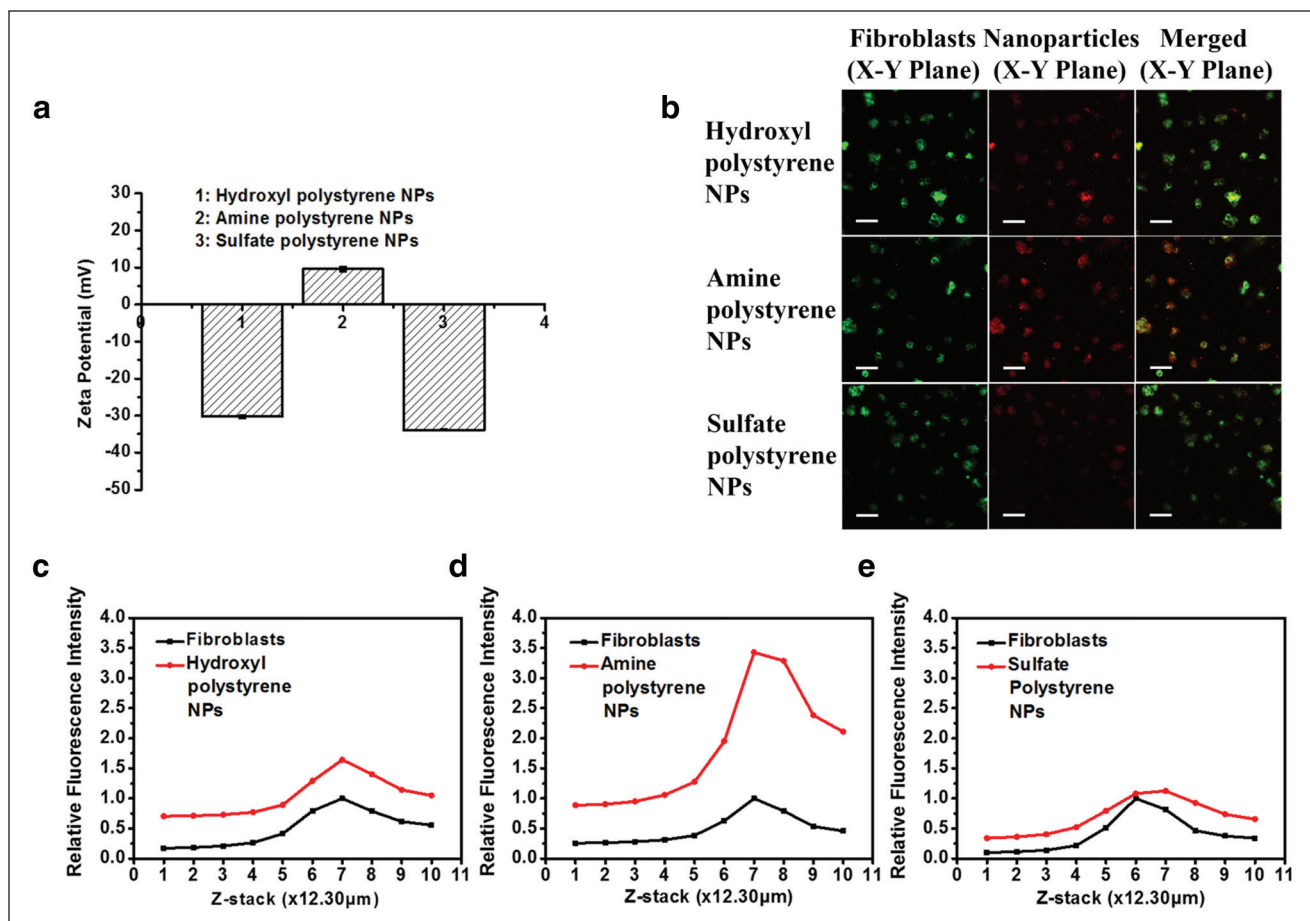


Figure 5. Constructs of fibroblast-laden collagen for examining the skin penetration capability of polystyrene NPs with different surface charges. (a) Zeta potential of polystyrene NPs of the same size (100 nm) but with different surface coating (hydroxyl, amine, or sulfate). (b) Confocal images of fibroblasts in the 3D constructs after being labeled with polystyrene NPs (red) for 3 h. Cells were stained with DiO (green). Microscopy objective: 20 \times . Scale bar: 100 μ m. Relative fluorescence intensity of each stack of the 3D constructs by normalizing the green or red signal against the green signal of the cells in stack 7 of each 3D construct: (c) 3D constructs treated with hydroxyl polystyrene NPs, (d) 3D constructs treated with amine polystyrene NPs, and (e) 3D constructs treated with sulfate polystyrene NPs.

same size (100 nm) but with different surface coating (hydroxyl, amine, or sulfate) for 3 h. The different surface chemistry provided different surface charges; hydroxyl polystyrene NPs and sulfate-modified polystyrene NPs were negatively charged, while amine-modified polystyrene NPs had a positive surface potential (Fig. 5a).

After 3 h of incubation, the constructs were examined with confocal imaging. As shown in Figure 5b, cells in the construct treated with amine-modified polystyrene NPs showed higher fluorescence intensity than the other two samples. As cells in all constructs were prelabeled with the cell tracker (i.e., DiO), the fluorescence signal from the NPs (red) in each cell was normalized against the cell tracker signal (green) from the same cell. For samples treated with hydroxyl polystyrene NPs, amine polystyrene NPs, and sulfate polystyrene NPs, the ratios were 1.7, 3.5, and 1.2, respectively (value of red lines at stack 7 in Fig. 5c–e). In

other words, the penetration efficiency of amine-modified polystyrene NPs through the collagen gel to reach the cell layer is about twofold that of the other two polystyrene NPs. This observation is consistent with a previous study. Ryman-Rasmussen et al. had examined the influence of surface charges of quantum dots on the skin penetration by using quantum dots coated with polyethylene glycol (neutral), polyethylene glycol-amine (cationic), and carboxylic acid (anionic). They discovered that cationic charged quantum dots could penetrate deeper into the skin (dermal layers) than their neutral and anionic counterparts (epidermis layer) within 8 h,¹⁶ which might be explained by the electrostatic repelling between the negatively charged skin and negatively charged NPs, resulting in the aggregation of the NPs, and further impacting their penetration ability.¹⁷

We further probed into the green fluorescence signal at the different stacks of the 3D construct and observed that all

three samples showed similar green signal distribution patterns (black lines in **Fig. 5c–e**). Specifically, the green signal intensities at stacks 5–8 were significantly stronger than those at stacks 1–4 and 9–10. This indicates that DiO-labeled cells were located between stacks 5–8. For the NP signal, a similar trend was observed. Stacks containing cells showed an obvious and stronger NP fluorescence signal than other stacks, although samples treated with amine-modified polystyrene NPs manifested the highest signal intensity.

Conclusion

We have successfully developed an artificial skin model for rapid NP transdermal screening via a multilayer construct composed of collagen I and fibroblasts through 3D printing technology. Using the skin model, we examined the penetration efficacy of various surface-charged polystyrene NPs and found that the current skin model showed a penetration profile similar to that of a living dermal tissue. This affirms that the current 3D-printed artificial skin model is promising as a platform to explore mechanisms involved in transdermal drug delivery and to accelerate the screening process of therapeutic NPs in the skin care industry.

Declaration of Conflicting Interests

The authors declared no potential conflicts of interest with respect to the research, authorship, and/or publication of this article.

Funding

The authors disclosed receipt of the following financial support for the research, authorship, and/or publication of this article: The work was supported by the School of Chemical and Biomedical Engineering at Nanyang Technological University, NTU-Northwestern Institute for Nanomedicine at Nanyang Technological University, and National Natural Science Funds of China (Grant 81201190 to Chenjie Xu).

References

1. Prausnitz, M.; Mitragotri, S.; Langer, R. Current Status and Future Potential of Transdermal Drug Delivery. *Nat. Rev. Drug Discov.* **2004**, *3*, 115–124.
2. Dianzani, C.; Zara, G.; Barrera, G.; et al. Drug Delivery Nanoparticles in Skin Cancers. *Biomed. Res. Int.* **2014**, *2014*, 1–14.
3. Bonini, M.; Berti, D.; Baglioni, P. Nanostructures for Magnetically Triggered Release of Drugs and Biomolecules. *Curr. Opin. Colloid Interface Sci.* **2013**, *18*, 459–467.
4. Amstad, E.; Reimhult, E. Nanoparticle Actuated Hollow Drug Delivery Vehicles. *Nanomedicine (Lond.)* **2012**, *7*, 145–164.
5. Preiss, M.; Bothun, G. Stimuli-Responsive Liposome-Nanoparticle Assemblies. *Expert Opin. Drug Deliv.* **2011**, *8*, 1025–1040.
6. Elliott, N.; Yuan, F. A Review of Three-Dimensional In Vitro Tissue Models for Drug Discovery and Transport Studies. *J. Pharm. Sci.* **2011**, *100*, 59–74.
7. Zein, I.; Hutmacher, D.; Teoh, S.; et al. Fused Deposition Modeling of Novel Scaffold Architectures for Tissue Engineering Applications. *Biomaterials* **2002**, *23*, 1169–1185.
8. Matsusaki, M.; Kadowaki, K.; Nakahara, Y.; et al. Fabrication of Cellular Multilayers with Nanometer-Sized Extracellular Matrix Films. *Angew. Chem. Int. Ed.* **2007**, *46*, 4689–4692.
9. Lee, W.; Debasitis, J.; Yoo, S.; et al. Multi-Layered Culture of Human Skin Fibroblasts and Keratinocytes through Three-Dimensional Freeform Fabrication. *Biomaterials* **2009**, *30*, 1587–1595.
10. Lee, W.; Lee, V.; Yoo, S.; et al. Three-Dimensional Cell-Hydrogel Printer Using Electromechanical Microvalve for Tissue Engineering. *Transducers 2009*, Denver, CO, June 21–25, 2009.
11. Lee, V.; Singh, G.; Karande, P. Design and Fabrication of Human Skin by Three-Dimensional Bioprinting. *Tissue Eng. Part C Methods* **2014**, *20*, 473–484.
12. Xu, C.; Miranda-Nieves, D.; Ankrum, J. A.; et al. Tracking Mesenchymal Stem Cells with Iron Oxide Nanoparticle Loaded Poly(lactide-co-glycolide) Microparticles. *Nano Lett.* **2012**, *12*, 4131–4139.
13. Breitzkreutz, D.; Mirancea, N.; Nischt, R. Basement Membranes in Skin: Unique Matrix Structures with Diverse Functions? *Histochem. Cell. Biol.* **2009**, *132*, 1–10.
14. Fitzgerald, K.; Guo, J.; O'Driscoll, C.; et al. The Use of Collagen-Based Scaffolds to Simulate Prostate Cancer Bone Metastases with Potential for Evaluating Delivery of Nanoparticulate Gene Therapeutics. *Biomaterials* **2015**, *66*, 53–66.
15. Faulkner-Jones, A.; Greenhough, S.; Shu, W.; et al. Development of a Valve-Based Cell Printer for the Formation of Human Embryonic Stem Cell Spheroid Aggregates. *Biofabrication* **2013**, *5*, 1–13.
16. Ryman-Rasmussen, J.; Riviere, J.; Monteiro-Riviere, N. Penetration of Intact Skin by Quantum Dots with Diverse Physicochemical Properties. *Toxicol. Sci.* **2006**, *91*, 159–165.
17. Shanmugam, S.; Song, C.; Yoo, B.; et al. Physicochemical Characterization and Skin Permeation of Liposome Formulations Containing Clindamycin Phosphate. *Arch. Pharm. Res.* **2009**, *32*, 1067–1075.